FIRST OPERATION OF THE FERMI@ELETTRA BUNCH LENGTH MONITOR SYSTEM

M. Veronese*, R.Appio, T.Borden, G.Ciani, P.Craievich, R. De Monte,
S. Di Mitri, M. Ferianis, G.Gaio, S.Grulja, G.Scalamera, M.Tudor Sincrotrone Trieste, Trieste, Italy

Abstract

Both absolute and relative bunch length measurement are key information for FERMI@Elettra commissioning and operation. In this paper we present the relative Bunch Length Monitor (BLM) system that has been designed and implemented at Sincrotrone Trieste. The first BLM station has been installed downstream the first bunch magnetic compressor (BC1) of FERMI@Elettra. In this paper we report about the first operation of the BLM system; it is based on the power measurement of the coherent radiations. To allow for efficient performances in the extended range of the foreseen bunch lengths for FERMI@Elettra, the system has adopted a pyrodetector for coherent edge radiation from the last dipole. Also, the coherent diffraction radiation generated in a ceramic gap located downstream of BC1 is detected by a set of mm-wave diodes. The design of the system, along with its layout, is presented as well as the first measurement results obtained from the FERMI@Elettra compressed bunches.

MACHINE PARAMETERS

FERMI@Elettra is a single pass seeded FEL under construction at the Sincrotrone Trieste Laboratory. It is based on a UCLA photoinjector gun with design emittance of 2 mm mrad and charge per bunch in the range from 0.1nC to 1nC. The normal conducting Linac will operate at 50Hz delivering a final beam energy of 1.5GeV. Two bunch compressors (BC1 and BC2) will compress the bunch length in a range from 5ps to 0.15ps FW. The two FEL chains (FEL1 and FEL2) are designed to cover a total range from 100nm to 10nm delivering peak power of the order of GWs. A description of the facility is presented in the FERMI Conceptual Design Report [1]. Longitudinal diagnostics are of crucial importance to meet the FERMI@Elettra needs in term of performances. Two Bunch Length Monitors (BLM) are foreseen, one at the exit of each bunch compressor. The BLM will provide the relative bunch length information required by the longitudinal feedback system. The bunch length infomation is needed to stabilize the final output peak power of the FELs by stabilizing the electron beam peak current.

* marco.veronese@elettra.trieste.it

BLM LAYOUT

The FERMI@Elettra BLM has been designed to allow for relative bunch length measurements in a range from 5 ps to 0.15 ps FW (flat top current profile). To allow for this very wide range of bunch lengths two coherent radiation sources are used. The first source is the coherent radiation from the bending magnets of the BC1 compressor. The second is coherent radiation from a ceramic gap. The diagnostics based on the first source covers the range from 1ps to 0.15 ps FW, being its transfer function limited at low frequencies by angular acceptance of the transport system and by the sensitivity of the pyrodetectors. The rest of the range, i.e. from 1 ps to 5 ps FW, is covered by the system based on the radiation emitted from the gap. The separation of these ranges is more a matter of best performances than a net boundary between the detection capability of the two systems. The design has greatly benefited from LCLS BLM and ceramic gap based diagnostics [2].
The system is shown in figure 1 with the electron beam ideally moving from left to right.

The vacuum chamber is composed of a cube connected

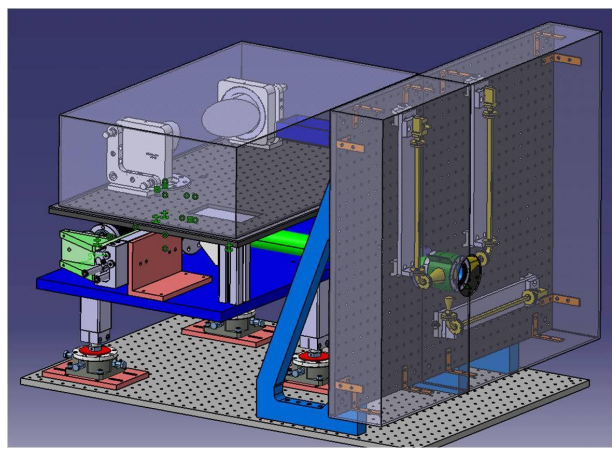

Figure 1: Bunch Length Monitor layout.

immediately downstream the last dipole of the bunch compressor. It houses an holey mirror that reflects the radiation upwards to a collimating-focusing pair of off axis parabolic mirrors. The first mirror is needed to collimate the radiation while the second is used to focus it onto a pyrodetector. A z-cut quartz window is used to separate the vacuum from the atmosphere. A dry air purgeable enclosure surrounds both mirrors and pyrodetector. The gap system is installed immediately downstream and the

detection is performed by three mm-wave diodes with central frequencies around respectively 30, 100 and 300 GHz. The diodes are mounted on a optical breadboard by means of translation stages that allow to vary the distance of the diode from the gap.

COHERENT RADIATION FROM THE DIPOLES

A detailed study of CSR-CER radiation properties has been performed using the *Synchrosym* code [3] based on the Liénard Wiechert potentials:

.

$$\vec{E} = \frac{e}{4\pi\epsilon_0}\left\{\frac{(\vec{n}-\vec{\beta})}{\gamma^2(1-\vec{n}\vec{\beta})^3R^2} + \frac{\vec{n}\times((\vec{n}-\vec{\beta})\times\vec{\beta})}{c(1-\vec{n}\vec{\beta})^3R}\right\} \quad (1)$$

The code is capable to handle the emission from an arbitrary magnetic field profile and evaluated both velocity and acceleration terms and also include mirror charges.

Figure 2 show the total intensity on the detector including

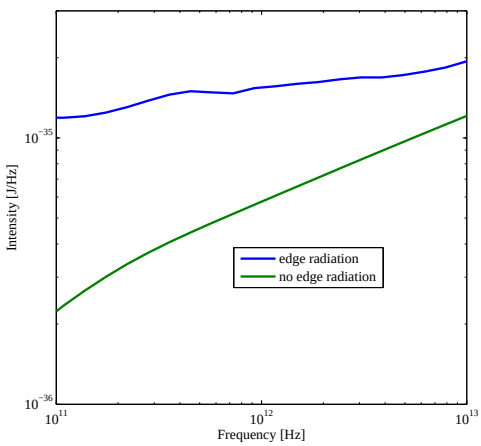

Figure 2: Spectral dependence of the radiation emitted from the last dipole of BC1. The blue curve includes velocity term that dominated for edge radiation while the green is classical synchrotron radiation.

the effect of the 3rd and 4th dipoles and both velocity and acceleration terms, compared to the classical synchrotron radiation emission. It can be clearly seen that at low frequency the radiation is strongly dominated by edge radiation while at higher frequencies the pure synchrotron radiation component become almost comparable. Moreover a small but not negligible contribution from radiation coming from the 3rd dipole is expected.

The optimization of the system includes an analysis of the spectral transmission of the whole transport systems. Limitations in the transmission for low frequencies arise from geometrical apertures. Longer wavelength radiations are emitted at larger angles thus apertures create low frequency cutoffs. At high frequencies the limitations arise from the transmission of the vacuum windows used to extract the radiation and from water absorption related to humidity in the air. For this reasons we decided to use z-cut crystal quartz as the window material which guarantees transmission up to about 3 THz and is transparent in the visible, allowing an optical alignment of the mirrors. To reduce the impact of humidity the window, the mirrors and the detector are separated from the rest of the atmosphere by a sealed enclosure. A dry air purging system is capable to reduce the relative humidity (RH) in the enclosure from an ambient RH of 45% to a value of about 1% in less than 20 minutes. In the range of bunch length so far explored the suppression of humidity lead to an improvement of about 10% in the total energy transmission of the system.

Figure 3 shows the spectral dependence of the optical transmission of the system at the pyrodetector. The code from H. Loos has been used to optimize the apertures diameter, the distances and the size of the mirrors to allow for optimal radiation collection from 300 GHz to 10THz. The low frequency cutoff is mainly due to the

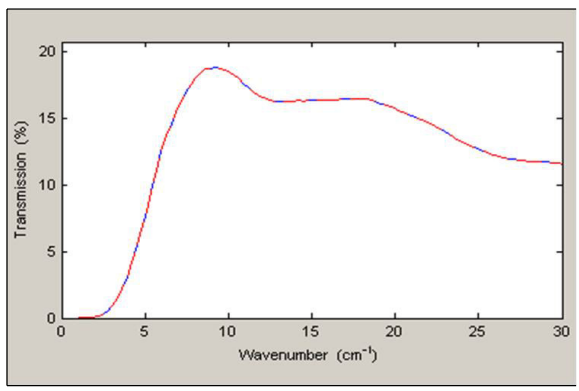

Figure 3: Spectral dependence of the transmission of the optical system.

limited initial angular acceptance caused by mechanical constraints and only partially due to diffraction at the detector.

COHERENT RADIATION FROM A CERAMIC GAP

The problem of the radiation emission of an ultrarelativistic particle can be studied starting from Maxwell equations, with the introduction of boundary conditions. We follow the approach of Bolotowskii [4] and Palumbo [5]. For the evaluation of the electromagnetic field it is convenient to introduce the Hertz potential Π, in relation to which the fields are:

$$\mathbf{E} = \nabla\nabla\cdot\mathbf{\Pi} - \frac{\mathbf{1}}{\mathbf{c^2}}\frac{\partial^\mathbf{2}\mathbf{\Pi}}{\partial\mathbf{t^2}}, \mathbf{H} = \frac{\mathbf{1}}{\mathbf{c}}\nabla\times\frac{\partial\mathbf{\Pi}}{\partial\mathbf{t}} \quad (2)$$

and is related to **p**, the polarization density, by the equation:

$$\frac{\partial^2 \mathbf{\Pi}}{\partial r^2} + \frac{1}{r}\frac{\partial \mathbf{\Pi}}{\partial r} + \frac{\partial^2 \mathbf{\Pi}}{\partial z^2} - \frac{1}{c^2}\frac{\partial^2 \mathbf{\Pi}}{\partial t^2} = -4\pi \mathbf{p} \qquad (3)$$

A point charge moving in a discontinue circular waveguide of radius a induces currents on the walls of the guide. At a boundary with free space, the currents become sources for an electromagnetic field radiating in the surrounding space. The evaluation of the radiated field can be performed with the help of *Wiener-Hopf factorization method*. The exact solution of the electromagnetic problem, including interferences between the two faced guides has been found in [5]. This result has been recently applied to electron beam diagnostics [6].

For brevity, we report in equation 4 the final expression for the single particle spectrum angular distribution, considering the structure in a spherical coordinate system (R, θ, ϕ) superimposed on a cylindrical coordinate system (r, ϕ, z). For an infinite circular waveguide, with a gap having semilength ℓ, if the charge travels along the axis of the waveguide, the Wiener-Hopf method leads to:

$$\begin{aligned}\frac{d^2W(\theta)}{d\omega d\Omega} &= \beta q^2 \frac{\sin^2\theta J_0^2(ka\sin\theta)}{4\pi^2 c(1-\beta\cos\theta)^2 I_0^2(\frac{ka}{\beta\gamma})} \\ &\left| \frac{L^-(\omega/v)\sqrt{1-\beta}e^{jk\ell(1-\beta\cos\theta)/\beta}}{L^-(k\cos\theta)\sqrt{1-\cos\theta}} + \right. \\ &\left. j\frac{L^+(\omega/v)\sqrt{1+\beta}e^{-jk\ell(1-\beta\cos\theta)/\beta}}{L^+(k\cos\theta)\sqrt{1+\cos\theta}} \right|^2 \end{aligned} \qquad (4)$$

where β is the ratio v/c, k is the wavenumber, a is the radius of the pipe. The functions $L^+(\alpha)$ and $L^-(\alpha)$ come from the factorization of the kernel:

$$L(\alpha) = \pi a \Omega J_0(\Omega a) H_0^{(1)}(\Omega a) \qquad (5)$$

where $J_0(x)$ is the first type, zero order Bessel function, and $H_0^{(1)}(x)$ is the Hankel function, while $\Omega = \sqrt{k^2 - \alpha^2}$. The expression for these functions is obtained in [7]. For high frequencies, the approximation $L^+(\alpha) = L^-(\alpha) \approx 1$ can be performed, obtaining:

$$\begin{aligned}\frac{d^2W(\theta)}{d\omega d\Omega} &= \beta q^2 \frac{\sin^2\theta J_0^2(ka\sin\theta)}{4\pi^2 c(1-\beta\cos\theta)^2 I_0^2(\frac{ka}{\beta\gamma})} \\ &\left| \sqrt{\frac{1-\beta}{1-\cos\theta}} e^{jk\ell(1-\beta\cos\theta)/\beta} + \right. \\ &\left. j\sqrt{\frac{1+\beta}{1+\cos\theta}} e^{-jk\ell(1-\beta\cos\theta)/\beta} \right|^2 \end{aligned} \qquad (6)$$

For ultrarelativistic charged particles, the first term ("step-in") in the absolute value of eq 6 tends to zero, and the gap emission is dominated by the second term, representing emission from "step-out". Figure 4 shows the spectrum-angular density of the energy radiated versus the frequency, for both incoming and outgoing particle cases, for a 250 MeV electron. From this figure it can be noted that the radiation from an outgoing particle is several orders of magnitude greater than the one due to an incoming particle. The minima are related to the $J_0^2(ka\sin\theta)$ function in equation 6, typical of diffraction radiation from hole, and their position in frequency is independent from the beam energy.

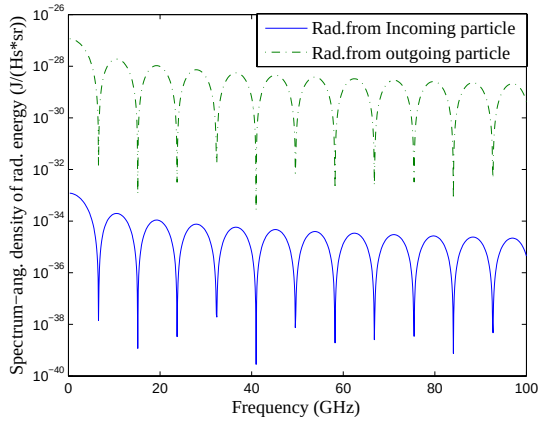

Figure 4: Spectrum-angular density of the energy radiated by a 250 MeV charge entering and going out from a semi-infinite waveguide versus frequency, at an angle θ of $\pi/2$ rads from the pipe axis.

For a bunch of N electrons with a given longitudinal current profile, the coherent emission from the gap can be calculated. Figure 5 shows the energy radiated by a rectangular electron bunch passing through the gap, for different bunch lengths. It can be noted that the system sensitivity is greater for longer bunches, while for shorter and shorter bunches, the radiated energy in a fixed bandwidth does not significantly change. To obtain the total energy radiated by

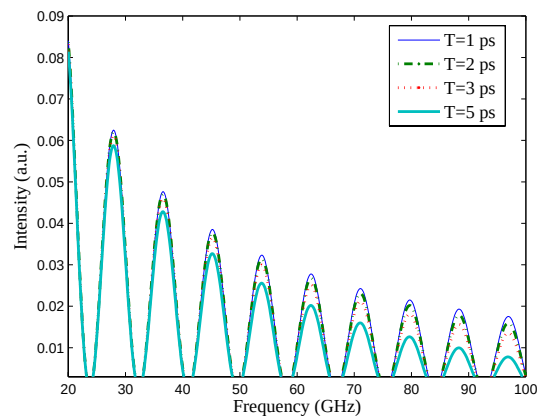

Figure 5: Spectrum-angular density of energy radiated by a rectangular electron bunch passing through a gap in a waveguide, calculated for different bunch lengths, and for a bunch energy of 250 MeV. The density has been calculated at an angle θ of $\pi/2$ rads from the pipe axis.

the bunch in the GAP region, one needs to integrate the spectrum-angular density over the frequency and over the total solid angle of radiation.

MEASUREMENTS

During the first operation of the BLM system, several measurements have been performed to characterize the system response. In the following we show BLM signals acquired varying the compression factor of BC1, by changing the phase of the previous linac section while keeping the bending angle fixed. In the Figures 6 and 7 we show the measurements performed at 0.085 rads.

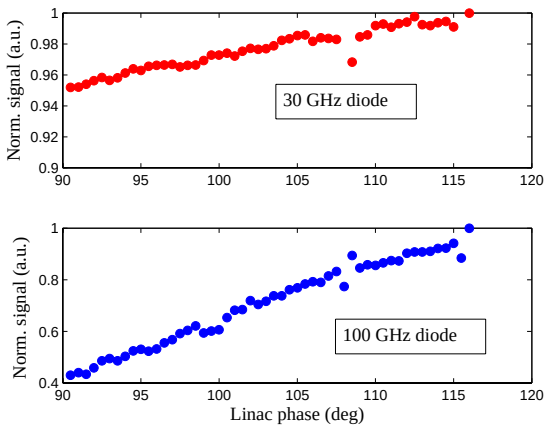

Figure 6: Signals of the 30GHz and 100GHz diodes vs linac 1 phase.

As expected from the theory and shown in figure 5 the sensitivity of the gap radiation detection system is higher for the diode operating at frequencies of 100 GHz while it is smaller for the 30GHz diode. Moreover going more off crest, thus compressing to shorter bunches, the signal increase rate is reduced. This can be qualitatively understood in terms of the longitudinal form factor that in this low frequency region does not change any more when the bunch length becomes very short. Finally for both detectors, a signal is detected also for uncompressed beam corresponding to a bunch length FW of 6ps.

The pyrodetector signal vs phase, shown in figure 7 becomes detectable only when the bunch becomes short enough, that is at about a bunch length of 1.5ps FW. Concerning the detection performances in terms of signal to noise ratio, which is one of the key point in their use for feedback systems, the diodes show very good performances. The signal from the 30GHz diode having a SNR of 1.5% rms, the 100GHz diode being around 2 % rms. For the pyrodetector the SNR is significantly higher, i.e. around 10 % rms.

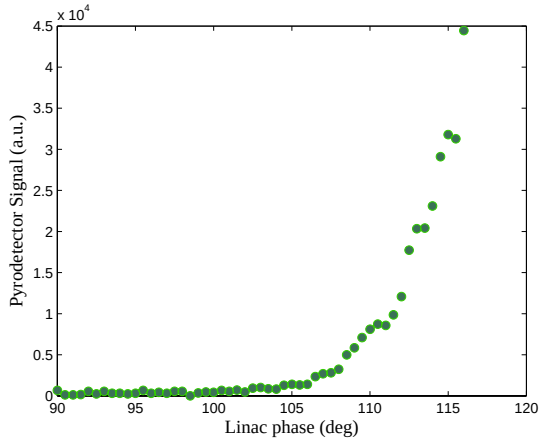

Figure 7: Pyrodetector signal vs linac 1 phase.

CONCLUSIONS

We have reported on the final design and the first operation of the FERMI Bunch Length Monitor. A description of the system has been provided both for coherent radiation from the dipoles and for radiation from a ceramic gap. Performances in terms of sensitivity and signal to noise ratio are discussed.

ACKNOWLEDGMENTS

The authors would like to thank H. Loos and J. Frish for precious discussions and for providing the Matlab code used to simulate the transport for the CER radiation and insight in ceramic gap diagnostics and mm-wave diodes as well as pyrodetectors. O. Grimm for providing his *Synchrosim* code and L. Palumbo for the very useful discussion on the gap emission theory. Finally we would like to thank R.Sauro and R.Tamaro for their support.

REFERENCES

[1] Conceptual Design report FERMI@Elettra http://www.elettra.trieste.it/FERMI/

[2] H.Loos *etal*. Proceedings of PAC07, pg 4189, 2007.

[3] O. Grimm, TESLA-FEL Report 2008-05

[4] G. Voskresenskii and B. Bolotovskii, Soviet Physics-Technical Physics, 9(4), October 1964.

[5] L.Palumbo, Technical Report, CERN-LEP-TH/84-4, Geneve, 1984

[6] T.Suwada and M.Satoh, Proceedings of LINAC08, pg 584, 2008

[7] L.Weinstein, *The Theory of Diffraction and the Factorization Method (Generalized Wiener-Hopf Technique)*, Golem Series in Electromagnetics, Boulder, Colorado, 1969.